

Active Galactic Nuclei and the Truncation of Star Formation in K+A Galaxies

Michael J. I. Brown¹, John Moustakas^{2,3}, Nelson Caldwell⁴, David Palamara¹, Richard J. Cool^{5,6,7}, Arjun Dey⁸, Ryan Hickox⁹, Buell T. Jannuzi⁸, Stephen S. Murray⁹, Dennis Zaritsky⁵

Michael.Brown@sci.monash.edu.au

ABSTRACT

We have searched for active galactic nuclei (AGNs) in K+A galaxies, using multiwavelength imaging and spectroscopy in the Boötes field of the NOAO Deep Wide-Field Survey. The K+A galaxies, which have had their star formation rapidly truncated, are selected via their strong Balmer absorption lines and weak $H\alpha$ emission. Our sample consists of 24 K+A galaxies selected from 6594 $0.10 < z < 0.35$ galaxies brighter than $I = 20$ with optical spectroscopy from the AGN and Galaxy Evolution Survey. Two thirds of the K+A galaxies are likely ongoing galaxy mergers, with nearby companion galaxies or tidal tails. Galaxy mergers may be responsible for the truncation of star formation, or we are observing the aftermath of merger triggered starbursts. As expected, the optical colors of K+A galaxies largely fall between blue galaxies with ongoing star formation and red passive galaxies. However, only 1% of the galaxies with colors between the red and blue populations are K+A galaxies, and we conclude that the truncation of star formation in K+A galaxies must have been unusually abrupt ($\lesssim 100$ Myr). We examined the AGN content of K+A galaxies with both optical emission-line ratios (BPT diagrams) and *Chandra* X-ray imaging. At least half of all K+A galaxies display the optical emission-line ratios of AGNs, and a third of $M_R < -22$ K+A galaxies host AGNs with X-ray luminosities of $\sim 10^{42}$ erg s⁻¹. The faintest K+A galaxies do not show clear evidence for hosting AGNs, having emission-line ratios consistent with photoionization by massive stars and few X-ray detections. We speculate that two mechanisms may be responsible for the truncation of star formation in K+A galaxies, with AGN feedback only playing a role in $M_R \lesssim -20.5$ galaxies.

Subject headings: galaxies: active – galaxies: evolution – galaxies: individual (IRAS 14344+3451) – galaxies: interactions – X-rays: galaxies

1. INTRODUCTION

The stellar mass contained within the red galaxy population has doubled over the past 7 Gyr (e.g., Bell et al. 2004; Brown et al. 2007; Faber et al. 2007). Almost all red galaxies have low specific star formation rates (e.g., Fukugita et al. 2004; Helmboldt, Walterbos, & Goto 2008), so this rapid stellar mass growth cannot re-

sult from in-situ star formation alone. Mergers of red galaxies can redistribute, but not significantly increase, the stellar mass within the red galaxy population. For the stellar mass to rapidly increase within the red galaxy population, stellar mass must be transferred from the blue galaxy population to the red galaxy population (Bell et al. 2004). For this to happen, star formation must be truncated within blue galaxies.

Galaxies that have had their star formation abruptly truncated within the past several hundred million years can be identified spectroscopically (e.g., Dressler & Gunn 1983; Boroson & Oke 1984; Couch & Sharples 1987; Zabludoff et al. 1996). These galaxies, which lack massive OB stars but retain longer lived A stars, have weak nebular emission-lines (relative to star forming galaxies) and a prominent Balmer absorption series. These galaxies are commonly known as post-starbursts (e.g Couch & Sharples 1987), E+A galaxies (e.g Dressler & Gunn 1983), or K+A galaxies (e.g Franx 1993), as their stellar continuum can be approximated by combining K and A star spectra.

There are several plausible mechanisms for the rapid truncation of star formation in galaxies, including strangulation (Larson, Tinsley, & Caldwell 1980; Balogh &

arXiv:0907.3185v1 [astro-ph.GA] 18 Jul 2009

¹School of Physics, Monash University, Clayton, Victoria 3800, Australia

²Center for Astrophysics and Space Sciences, University of California, San Diego, 9500 Gilman Drive, La Jolla, California, 92093-0424

³Center for Cosmology and Particle Physics, 4 Washington Place, New York University, New York, NY 10003

⁴Smithsonian Astrophysical Observatory, 60 Garden Street, Cambridge, MA 02138

⁵Steward Observatory, University of Arizona, 933 North Cherry Avenue, Tucson, AZ 85721

⁶Princeton University Observatory, Peyton Hall, Ivy Lane, Princeton, NJ 08544

⁷Hubble Fellow

⁸National Optical Astronomy Observatory, Tucson, AZ 85726-6732

⁹Harvard-Smithsonian Center for Astrophysics, Cambridge, MA 02138

Morris 2000), supernova feedback (e.g., Efstathiou 2000), virial shock heating (Dekel & Birnboim 2006) and feedback from active galactic nuclei (AGNs; e.g., Silk & Rees 1998; Wyithe & Loeb 2003; Bower et al. 2006; Croton et al. 2006; Hopkins et al. 2006a). Models incorporating AGN feedback have achieved prominence within the past decade, as they can reproduce the observed properties of low redshift galaxies (e.g., Bower et al. 2006; Croton et al. 2006; Hopkins et al. 2006b) and there is strong observational evidence for AGN feedback in nearby galaxy clusters (e.g., Fabian et al. 2003a, 2003b). However, galaxy models with AGN feedback can have more free parameters than competing models and while AGN activity is relatively easy to detect, proving that it is (solely) responsible for truncating star formation is non-trivial.

AGN host galaxies have been studied for decades, and while the primary goal of these studies is understanding what triggers AGN activity, such studies can also explore the connections between AGN activity and star formation. Examples of quasars with K+A host galaxies are well known (Boroson & Oke 1984; Brotherton et al. 1999, 2004), although there are also powerful AGNs hosted by starbursts (e.g., Gallagher et al. 2002) and AGNs hosted by galaxies with old stellar populations (e.g., Nolan et al. 2001). While the presence of powerful AGNs in star forming galaxies could be evidence for AGN feedback playing a negligible role in galaxy evolution, there are scenarios where AGN feedback only plays a significant role after millions of years of AGN activity (e.g., Hopkins et al. 2006a).

Recently there have been a number of studies of the AGN content of K+A galaxies, with the principal goal of determining if AGNs could plausibly truncate star formation. These studies suggest a correlation between AGN activity and the rapid truncation of star formation, although a causal link has yet to be established. K+A galaxies selected from the Sloan Digital Sky Survey (SDSS; York et al. 2000) typically have emission-line ratios comparable to LINERs (Low Ionization Nuclear Emission-line Regions; Heckman 1980) and Seyferts, consistent with AGN activity in these galaxies (Yan et al. 2006). A quarter of K+A galaxies have blue cores, and these cores have spectra similar to LINERs (Yang et al. 2006). Tremonti, Moustakas, & Diamond-Stanic (2007) observed Mg II $\lambda\lambda 2796, 2803$ absorption lines with blueshifts of $\sim 1000 \text{ km s}^{-1}$ in 10 of 14 $z \sim 0.6$ post-starburst galaxies, and hypothesized that these outflows were launched by AGNs that also truncated star formation within these galaxies. Stacking of *Chandra* images of $z \sim 0.8$ post-starburst galaxies reveals a population X-ray sources with a mean luminosity of $\sim 3 \times 10^{41} \text{ erg s}^{-1}$ (Georgakakis et al. 2008). These studies suggest a link between AGN activity and K+A galaxies.

In this paper, we examine the AGN content of $0.10 < z < 0.35$ K+A galaxies using the optical emission-line diagnostic diagrams of Baldwin, Phillips, & Terlevich (1981, BPT diagrams) and X-ray imaging with the *Chan-*

dra X-ray Observatory. Our principal goal is to measure the fraction of K+A galaxies that host AGNs, and thus determine if AGN feedback is a *plausible* mechanism for rapidly truncating star formation. We caution that even if all of the K+A galaxies in our sample host an AGN, this finding would be consistent with, but not direct evidence for, a causal link between AGN activity and the truncation of star formation. We also note that if none of the K+A galaxies in our sample host an AGN, one could develop models where the AGN activity is so brief that it would be rarely observed, although one may consider such models contrived. Despite these limitations and caveats, the plausibility of AGN feedback models does depend on the observed fraction of K+A galaxies that currently host AGNs.

The structure of this paper is as follows. In §2 we describe the selection of our K+A galaxy sample from the AGN and Galaxy Evolution Survey of Boötes. We discuss the NOAO Deep Wide-Field Survey optical imaging, photometry and rest-frame properties of the K+A galaxies in §3. The AGN content of K+A galaxies, inferred from optical emission line ratios and *Chandra* X-ray imaging is discussed in §4 and §5 respectively. We summarize our principal conclusions in §6. Throughout this paper we use Vega-based magnitudes and adopt a flat cosmology with $\Omega_m = 0.25$ and $H_0 = 72 \text{ km s}^{-1} \text{ Mpc}^{-1}$, which is consistent with the cosmological parameters of Spergel et al. (2007).

2. K+A GALAXY SAMPLE SELECTION

We selected our sample of K+A galaxies from the AGN and Galaxy Evolution Survey (AGES; C. S. Kochanek et al. in prep.), a spectroscopic survey of 7.9 deg^2 of the Boötes field of the NOAO Deep Wide-Field Survey (NDWFS; Jannuzi & Dey 1999). AGES targeted all optically extended sources brighter than $I = 18.5$ and $\gtrsim 20\%$ of extended sources with magnitudes of $18.5 < I < 20.0$. AGES also targeted other galaxies, using a variety of selection criteria (e.g., infrared colors), but we only include these objects in our *K + A* sample if they were also part of the main *I*-band selected galaxy sample.

The spectra were obtained with Hectospec, a 300-fiber robotic spectrograph with a 1° field-of-view on the 6.5-m MMT telescope (Fabricant et al. 1998; Roll, Fabricant, & McLeod 1998). The wavelength range of the spectra is $\simeq 3700 \text{ \AA}$ to $\simeq 9200 \text{ \AA}$, and the instrumental resolution is 6 \AA . Spectra were extracted and classified using two independent reduction pipelines and then verified by visual inspection. One pipeline is based upon the SDSS spectroscopic data reduction software while the other is a set of customized IRAF scripts. The spectra were flux calibrated by assigning several Hectospec fibers to F stars (identified from the SDSS; York et al. 2000), and then comparing their observed spectra with Kurucz (1992) stellar atmosphere models. To reliably select K+A galaxies using accurate measurements of galaxy emission and absorption lines, we require a median continuum signal-to-noise of 4 per pixel. We excluded spectra if they were

badly contaminated by a red light leak from an LED in the fiber positioner or suffered from poor flux calibration due to problems with the operation of the atmospheric dispersion corrector (even when reliable redshifts were possible).

To select K+A galaxies, we use the equivalent width of the $H\alpha$ emission-line and the Worthey & Ottaviani (1997) indices for the $H\delta$ and $H\gamma$ absorption lines. Our approach is similar to that used in much of the literature. K+A galaxies are identified by searching for spectra with strong Balmer absorption and weak nebular emission (e.g., [OII] $\lambda 3727$, $H\beta$, $H\alpha$) relative to star forming galaxies (e.g., Zabludoff et al. 1996; Quintero et al. 2004; Yan et al. 2008). While the selection criteria used in the literature are based on the same underlying principle, they vary in detail and select different samples of objects, and we return to this point later. The strength of the $H\alpha$ emission-line is a very strong function of the number UV photons produced by massive OB stars. If star formation is completely truncated in a galaxy after a period of star formation, the $H\alpha$ emission-line will disappear from the integrated galaxy spectrum within 10 Myr. The $H\delta$ and $H\gamma$ absorption lines are particularly strong in A star spectra, so these absorption lines remain prominent in galaxy spectra for ~ 300 Myr after the truncation of star formation.

Our principal selection criteria for K+A galaxies are

$$\begin{aligned} (H\delta_A + H\gamma_A)/2 > 3 \\ \log(H\alpha \text{ EW}) < 0.2 \times (H\delta_A + H\gamma_A)/2, \end{aligned} \quad (1)$$

where $H\delta_A$ and $H\gamma_A$ are the spectral indices of Worthey & Ottaviani (1997) and $H\alpha$ EW is the equivalent width of the $H\alpha$ emission-line (in units of \AA). Using the stellar population synthesis models of Bruzual & Charlot (2003) with Solar metallicity, we find that a galaxy that has had its star formation completely truncated after 10 Gyr of continuous star formation will meet our selection criteria for 300 Myr.

We caution that $H\alpha$ emission can also be produced by AGNs as well as star formation, and some K+A galaxies that host AGNs will be absent from our sample. For example, IRAS 14344+3451 (J2000 $R.A.=14:36:31.99$ $Decl.=+34:38:29.5$) is a $z = 0.349$ obscured quasar, hosted by a post-starburst galaxy undergoing a merger, that is excluded from our sample as it has strong $H\alpha$ emission. While one could attempt to add such objects to the sample by hand, this greatly complicates the selection function so we have stuck with a simple selection criterion that can be easily modeled. Our estimates of the fraction of K+A galaxies that host an AGN are thus lower limits.

In addition to our principal selection criteria, we employ a number of other criteria and techniques to reduce contamination and improve the sample definition. We limit our redshift range to $0.10 < z < 0.35$, so we have wavelength coverage of both the Balmer series and the emission-lines used in BPT diagrams. The lower redshift limit also reduces (but does not eliminate) aperture

bias, where a small and unrepresentative fraction of the galaxy flux enters the $1.5''$ Hectospec fiber. Measurements of $H\delta_A$ and $H\gamma_A$ can be corrupted by residuals from the 5577 \AA sky line, so we measure the strength of the Balmer absorption using only one of these indices when 5577 \AA (potentially) contaminates the other index. Measurement errors broaden the observed locus of star forming galaxies, so for spectra with a signal-to-noise per pixel between 4 and 8, we adopt the conservative selection criteria

$$\begin{aligned} (H\delta_A + H\gamma_A)/2 > 5 \\ \log(H\alpha \text{ EW}) < -0.2 + 0.2 \times (H\delta_A + H\gamma_A)/2. \end{aligned} \quad (2)$$

Contamination can be significant when selecting a very small subset of objects from a large population, so we visually inspected all of our K+A candidates and manually excluded 17 contaminants. Manually rejected objects included spectra with night sky line residuals and spectra where a red light leak had not been automatically flagged. Our selection criteria, K+A galaxies and other $I < 20$ galaxies are plotted in Figure 1. Of the 6954 I -band selected galaxies with $I < 20$, $0.10 < z < 0.35$ and good AGES spectra, 24 were selected as K+A galaxies. The low percentage (0.3%) of K+A galaxies in AGES is comparable to what has been observed in previous studies (e.g., Zabludoff et al. 1996; Quintero et al. 2004), even though the selection criteria differ. The coordinates and redshifts of the K+A galaxies are provided in Table 1 and we plot their spectra in Figure 2.

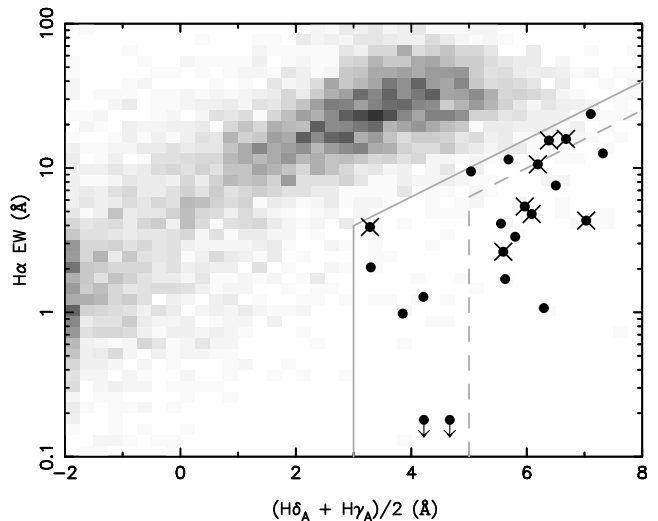


Fig. 1.— $H\alpha$ emission-line equivalent width as a function of the Worthey & Ottaviani (1997) indices for the $H\delta$ and $H\gamma$ absorption lines. Our selection criterion for spectra with a signal-to-noise of 8 (4) or more per pixel is shown with the solid (dashed) line. Our final sample of K+A galaxies is shown with the black circles, with *Chandra* sources highlighted with crosses. For comparison, the greyscale shows the distribution of I -band selected AGES galaxies with redshifts of $0.10 < z < 0.35$ and magnitudes of $I < 20$, including sources manually rejected from the post-starburst sample.

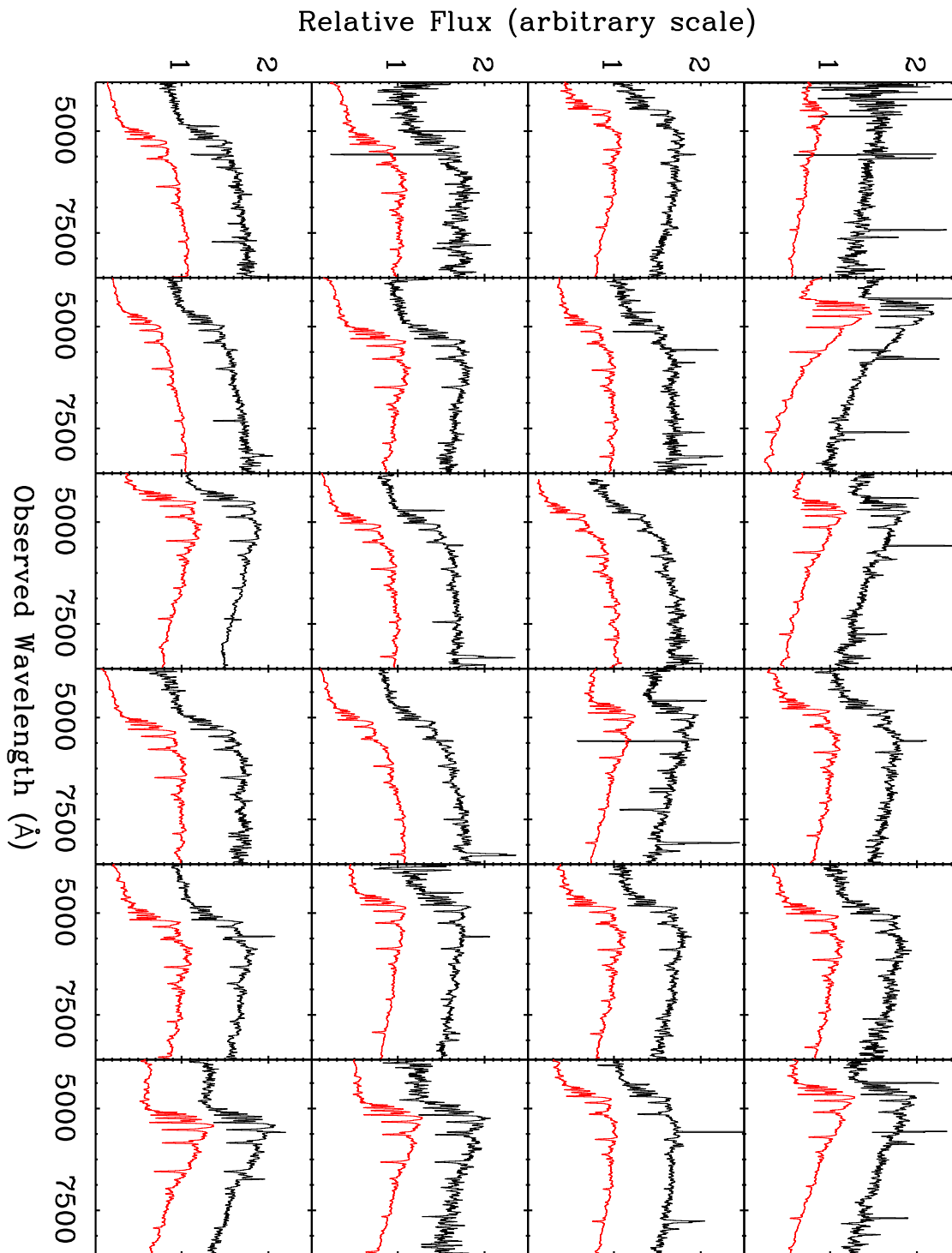


Fig. 2.— Spectra of the Boötes K+A galaxies. The spectra are listed in order of absolute magnitude, with the top row containing the faintest objects and the bottom row containing the brightest objects. In each panel we show the best-fit continuum model (red line) underneath the AGES spectrum (black line). Although many of the galaxies have nebular emission-lines, the equivalent widths of these lines are less than those of star forming galaxies with comparable Balmer absorption lines.

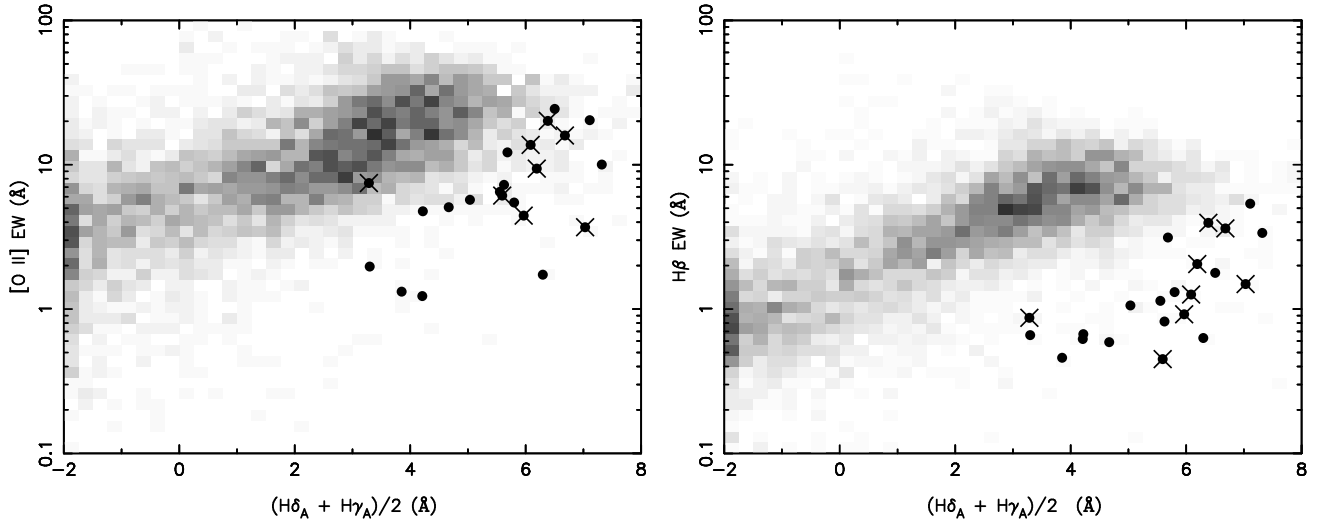


Fig. 3.— [O II] and H β emission-line equivalent width as a function of the Worthey & Ottaviani (1997) indices for H δ and H γ . Our final sample of K+A galaxies is shown with the black circles, with *Chandra* sources highlighted with crosses, while the greyscale shows the distribution of other $I < 20$ AGES galaxies with $0.10 < z < 0.35$. Many of our K+A galaxies have weak [O II] and H β relative to the locus of star-forming galaxies. However, some of our K+A galaxies have relatively strong [O II] or H β emission, and these objects would not have satisfied some of the K+A selection criteria used in the literature (e.g., Zabludoff et al. 1996).

A variety of K+A and post-starburst selection criteria are used in the literature. Consequently, there is a genuine concern that conclusions derived from one sample will not be applicable to other samples. To address (but not resolve) this concern, in Figure 3 we plot the equivalent width of the [O II] and H β emission-lines as a function of the H δ_A and H γ_A spectral indices. Our K+A galaxy sample has weak H β relative to the star-forming locus, and at least 80% of our objects would satisfy the H β selection criterion of Quintero et al. (2004). Although our K+A galaxies have weaker [O II] than galaxies in the star-forming locus, the difference is relatively small and $\sim 80\%$ of our K+A galaxies would be excluded from samples using the 2.5 \AA and 5 \AA [O II] emission-line equivalent width criteria of Zabludoff et al. (1996) and Tran et al. (2004) respectively. As noted by Yan et al. (2006), [O II] can result from AGN emission, and almost all of our K+A galaxies with X-ray counterparts (§5) would be excluded from samples using an [O II] selection criterion. Historically, [O II] was used not because it was preferred for physical reasons, but because detectors were more sensitive at those wavelengths. While our use of H α makes some comparisons with previous work more difficult, it is a good choice if one is more concerned about detecting recent star formation.

3. OPTICAL IMAGING AND PHOTOMETRY

To determine if galaxy mergers are associated with K+A galaxies, we searched for evidence of ongoing mergers using NDWFS optical imaging. As mergers are transitory, some galaxies that have undergone a merger within the past ~ 300 Myr may seem undisturbed in

the NDWFS imaging. As merger of two galaxies (initially separated by ~ 30 kpc) can take up to a billion years (e.g., Taylor & Babul 2001; Boylan-Kolchin, Ma, & Quataert 2008), merging K+A galaxies may be end products of merger triggered starbursts. While such caveats should be kept in mind, if a higher fraction of K+A galaxies are undergoing mergers than the overall galaxy population, this would be evidence for a link (albeit indirect) between K+A galaxies and galaxy mergers.

To determine if galaxy mergers play a role in the truncation of star formation, we searched the NDWFS optical imaging for companion galaxies within a projected distance of 30 kpc from each K+A galaxy. To reduce contamination of the companion sample, we used the photometric redshifts of Brown et al. (2008) to exclude companions whose photometric redshifts differed from the K+A galaxy spectroscopic redshifts by more than 0.2. We also excluded companion galaxies fainter than 10% of the K+A galaxy luminosity, as very faint galaxies can have large photometric redshift errors. An automated search of an object catalog will invariably miss some companion galaxies (e.g., due to blending) but is less likely to suffer from biases than visual searches. While only 17% of the overall AGES sample have companions within a projected distance of 30 kpc, we find that 8 (33%) of the 24 K+A galaxies have companion galaxies. The probability of randomly finding this enhanced number of companion galaxies is only 4%, so we conclude that K+A galaxies have more companions than the bulk of the galaxy population.

We also visually inspected NDWFS images of K+A galaxies for additional evidence of galaxy mergers, including tidal tails, and in Figure 4 we provide $20''$ I -band postage stamp images of the K+A galaxies. Ten (42%)

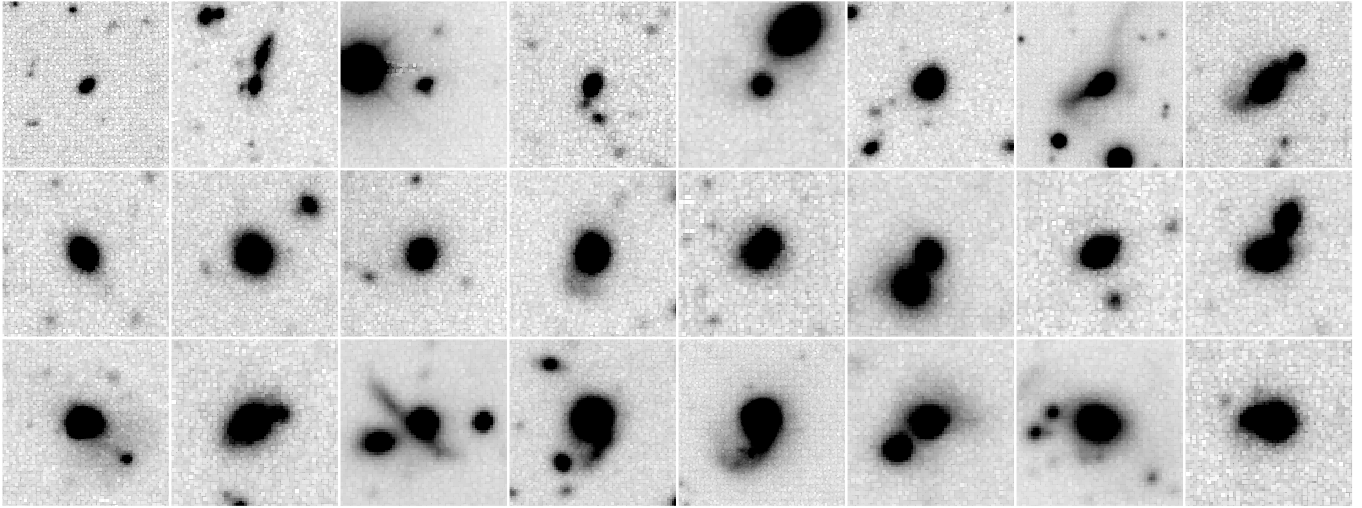


Fig. 4.— NDWFS I -band $20''$ field-of-view images of the K+A galaxies. As in Table 1, the objects are ordered by absolute magnitude, with faint objects in the top row and bright objects in the bottom row. We find that two thirds of the K+A galaxies show evidence for ongoing mergers, including nearby companion galaxies and tidal tails. All but one of the $M_R < -22$ K+A galaxies (bottom row) has a nearby companion galaxy or tidal tail.

of the K+A galaxies display tidal tails, including 7 that do not have companions within a projected distance of 30 kpc. The majority of K+A galaxies in our sample have nearby companion galaxies or tidal tails.

The high fraction of K+A galaxies undergoing mergers is broadly consistent with several previous studies, although these studies use a diverse range of galaxy selection criteria. Zabludoff et al. (1996) and Yang et al. (2008) find that a quarter and a half (respectively) of K+A galaxies show morphological evidence for ongoing mergers while Liu & Kennicutt (1995) found that a fifth of merging galaxies have K+A spectra. In contrast, Hogg et al. (2006) find that the environments of K+A galaxies do not differ from those of star-forming galaxies, although the SDSS sample used by Hogg et al. (2006) is too shallow to detect many of the companion galaxies we find using the deeper NDWFS imaging. While we find a higher fraction of merging K+A galaxies than prior studies, this is not unexpected as many K+A samples are small, the depth of their imaging varies, and the selection criteria for both K+A galaxies and mergers differ.

The fraction of merging K+A galaxies appears to increase with luminosity, with all but one of the eight $M_R < -22$ K+A galaxies having a tidal tail or a cataloged companion galaxy. However, the evidence is intriguing rather than conclusive. If the fraction of K+A galaxies undergoing mergers is 62% and does not vary with luminosity, then the probability that 7 of the 8 most luminous K+A galaxies in a sample would be undergoing mergers is 12%. Furthermore, some of the faintest K+A galaxies in our sample are undergoing mergers. It thus remains plausible that the K+A galaxy merger rate does not vary with optical luminosity.

We determined the apparent optical colors of our galaxies using copies of the NDWFS optical images smoothed to a common point spread function with a

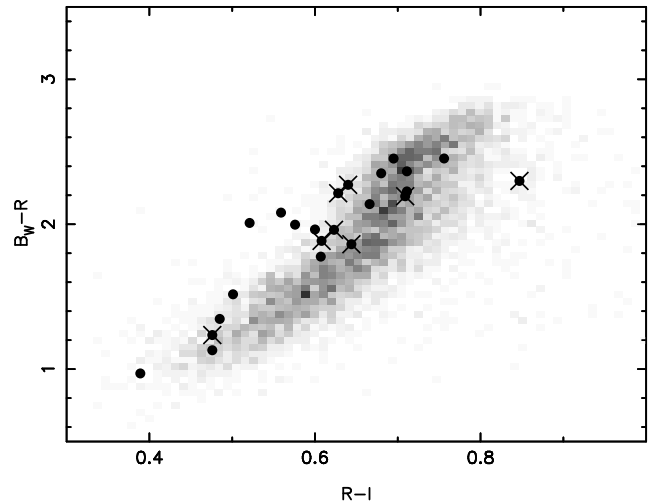


Fig. 5.— The apparent colors of $0.10 < z < 0.35$ K+A galaxies (black circles), K+A galaxies with X-ray counterparts (crosses) and other AGES galaxies (greyscale). One K+A galaxy has been excluded from the plot as its photometry is contaminated by a nearby bright star. The K+A galaxies have a broader spread of $B_W - R$ and $R - I$ colors than other galaxies, and it thus may be possible to select a large but incomplete sample of K+A candidates using apparent color criteria, although spectroscopy will still be required to produce a clean K+A sample.

FWHM of $1.35''$ and $8''$ aperture photometry (Brown et al. 2007). In Figure 5 we plot the apparent colors of our K+A galaxies and all $0.10 < z < 0.35$ AGES galaxies for comparison. We note that K+A galaxies have a broader spread of apparent colors than other AGES galaxies, which may be due to K+A galaxies having a prominent Balmer break rather than a strong 4000 \AA break. Others have noted that the colors of post-starbursts can differ from those of normal galaxies, and the K+A galaxies of Tremonti et al. (2007) were initially targeted (as quasar candidates) by the Sloan Digital Sky Survey for this reason. One may be able to isolate a large (albeit incomplete) sample of K+A galaxy candidates on the basis of their apparent colors and extended morphologies, although spectroscopy will still be required to obtain a clean K+A sample.

To determine the rest-frame photometry of our galaxies, we fitted Coleman, Wu, & Weedman (1980) template spectra to the optical photometry. To span the locus of galaxy colors, we interpolated between the Coleman et al. (1980) templates and extrapolated the templates to bluer and redder colors. We caution that the apparent colors of K+A galaxies do differ from those of most galaxies, so it is plausible that our rest-frame photometry for K+A galaxies has small systematic errors. For example, the Balmer break in K+A galaxies may have been incorrectly modeled with a 4000 \AA break during the SED fitting. In Figure 6 we plot rest-frame $U - V$ as a function of R -band absolute magnitude, which is strongly correlated with stellar mass. As seen in previous stud-

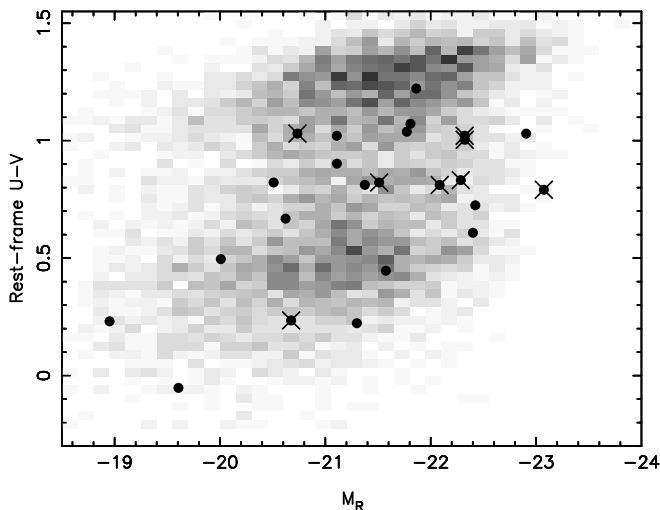


Fig. 6.— Rest-frame $U - V$ color as a function of R -band absolute magnitude. K+A galaxies (black circles) include some of the most and least luminous galaxies in the $0.10 < z < 0.35$ AGES sample. K+A galaxies with counterparts in the *Chandra* X-ray imaging (crosses) are, on average, more optically luminous than the bulk of the sample. As expected, K+A galaxies mostly fall between the red passive galaxies and the blue “cloud” of star forming galaxies, although K+A galaxies are a small minority of the galaxies in this color range.

ies (e.g., Quintero et al. 2004; Yan et al. 2008), most K+A galaxies have colors which fall between the “blue cloud” of star forming galaxies and the color-magnitude relation of red passive galaxies. This is not unexpected, as we have selected galaxies with negligible rates of star formation with stellar populations that are younger than those of red passive galaxies.

The stellar mass contained within the red galaxy population doubles between $z = 1$ and $z = 0$, due to steady transfer of stellar mass from the blue galaxy population to the red galaxy population (Bell et al. 2004; Brown et al. 2007; Faber et al. 2007). Consequently, many of the galaxies with intermediate colors must be in transition between the blue and red populations. We find that K+A galaxies represent just 1% of the 1984 $0.10 < z < 0.35$ AGES galaxies with high signal-to-noise spectra and restframe colors in the range $0.6 < U - V < 1.1$. If all galaxies moving between the blue and red populations had their star formation abruptly truncated ($< 300 \text{ Myr}$), so they satisfied K+A selection criteria, and it takes $\sim 1 \text{ Gyr}$ for the $U - V$ colors of galaxies to evolve from blue to red (e.g., Bell et al. 2004), we should have identified hundreds of K+A galaxies. Since we have only selected 24 K+A galaxies, we conclude that most of the galaxies falling between the red and blue populations at $z \sim 0.2$ have had their star formation decline gradually (so they do not meet K+A selection criteria). This interpretation is consistent with the recent work of Yan et al. (2008), who find that the slowly evolving environments of post-starbursts differ from those of most red galaxies. In contrast to our findings, Wild et al. (2009) find that K+A galaxies do play a significant role in transferring stellar mass from the blue population to the red population at $z \sim 0.7$, although this would require the space density of K+A galaxies to evolve by two orders of magnitude since $z = 0.7$. We conclude that while $z \sim 0.2$ K+A galaxies are in transition from the blue galaxy population to the red galaxy population, this transition seems to be atypical and unusually rapid for low redshift galaxies.

4. OPTICAL EMISSION-LINE FLUX RATIOS

The relative strength of emission-lines in a spectrum will vary depending upon the spectral energy distribution of the photo-ionizing radiation. As a consequence, emission line ratios can be used to distinguish AGNs from other galaxies (e.g., Baldwin et al. 1981; Kewley et al. 2001; Kauffmann et al. 2003), although there are caveats. The classifications derived from emission-line ratios can vary with the size of the aperture used when obtaining the spectrum (aperture bias; e.g., Zaritsky, Zabludoff, & Willick 1995), with weak AGNs being swamped by starlight in large aperture spectra. For most of the galaxies in our sample, the Hectospec fiber is capturing 10% to 30% of the total galaxy light, so the variation in aperture bias from galaxy-to-galaxy within our sample is small. Emission-line ratios also depend on

metallicity and the distributions of gas, dust and photoionizing sources. Despite these limitations, emission-line ratios remain a useful diagnostic of AGN content.

In this work we use the BPT diagram (Baldwin et al. 1981), which uses the emission-line flux ratios of [NII] $\lambda 6583$ divided by $H\alpha$ and [O III] $\lambda 5007$ divided by $H\beta$. Emission-line fluxes were determined by subtracting the stellar continuum and simultaneously fitting a Gaussian to each of the emission-line profiles (Moustakas & Kennicutt 2006, J. Moustakas, in prep.). This technique results in emission-line measurements reliably corrected for stellar absorption. The stellar continuum was modeled using a non-negative linear combination of high resolution Bruzual & Charlot (2003) stellar population synthesis models (which span a wide range of stellar population ages), with dust attenuation being modeled using the prescription outlined by Moustakas & Kennicutt (2006). With the AGES spectra, we are able to determine accurate emission-line fluxes when the line strength is greater than $\simeq 5 \times 10^{-17} \text{ erg s}^{-1} \text{ cm}^{-2}$. We note that the strength of the $H\alpha$ and $H\beta$ nebular emission-lines are sensitive to errors in the estimated strength of the Balmer absorption lines produced by the underlying stellar continuum model (§2). We also caution that an AGN can be missed if starlight and nebular emission dominates the light within the $1.5''$ aperture of the Hectospec fiber.

In Figure 7 we plot the BPT diagram of $0.10 < z < 0.35$ K+A galaxies and other AGES galaxies. For com-

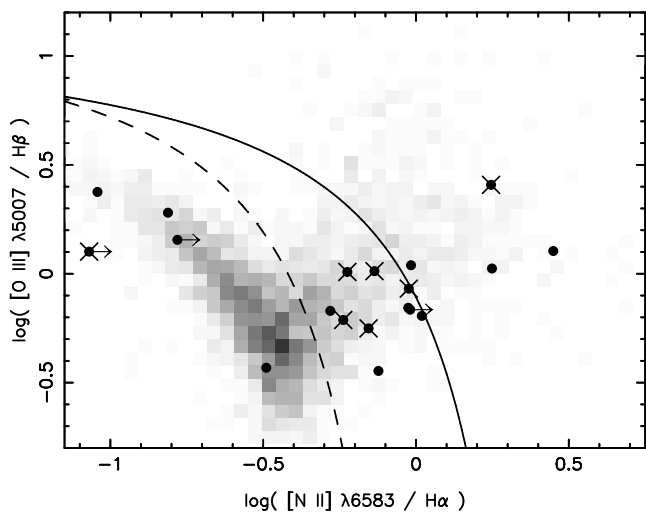


Fig. 7.— BPT diagram of K+A galaxies (black circles), K+A galaxies with X-ray counterparts (crosses), and other AGES galaxies (greyscale). For clarity we only plot those sources with 2σ emission-line detections or limits. The solid line is a theoretical upper limit for what can be produced by a stellar population (Kewley et al. 2001), while the dashed line is an empirical criterion used to distinguish AGNs from other galaxies (Kauffmann et al. 2003). The vast majority of our K+A galaxies lie in the AGN region of the BPT diagram defined using the Kauffmann et al. (2003) criterion.

parison, we plot the upper limit for the emission-line ratios produced by gas photoionized by massive stars from Kewley et al. (2001) and the empirical AGN criterion of Kauffmann et al. (2003). Clearly the K+A galaxy population differs significantly from the bulk of the galaxy population. Half of the K+A galaxies lie beyond the stellar population limit of Kewley et al. (2001), and the vast majority lie in the AGN portion of the BPT diagram defined with the Kauffmann et al. (2003) criterion. Our BPT diagram is broadly similar to that of Yan et al. (2006), except we have slightly fewer sources with strong [O III] $\lambda 5007$ emission relative to $H\beta$. While we are limited by small number statistics, it does appear that emission-line ratios may vary with optical luminosity. All three of the $M_R > -20.5$ K+A galaxies in our sample have $\log([\text{NII}] \lambda 6583 / H\alpha) \sim -1$, which is consistent with the nebular emission-line ratios produced by a stellar population. While it is possible that the $M_R > -20.5$ K+A galaxies are harboring weak AGNs that are swamped by starlight and associated nebular emission, or hosted powerful AGNs in the past, it is unlikely that these galaxies are currently hosting powerful AGNs. If the emission-line ratios measured by AGES are a reliable diagnostic of AGN activity, the fraction of K+A galaxies currently hosting an AGN increases with optical luminosity, with most $M_R < -20.5$ K+A galaxies hosting an AGN.

5. CHANDRA X-RAY IMAGING

AGNs which are not evident at optical wavelengths may be detected with X-ray imaging (e.g., Barger et al. 2001). The *Chandra X-ray Observatory* has imaged the entire Boötes field, with the lion's share of the imaging coming from the XBoötes wide-field and XBoötes deep surveys. We refer the reader to the XBoötes survey papers (Kenter et al. 2005; Murray et al. 2005; Brand et al. 2006; Murray & XBoötes Team 2006) for a thorough discussion of the observing strategy and data processing. The exposure time per pointing is at least 4 ks, with some regions of Boötes having exposure times as high as 172 ks (Wang et al. 2004). None of the K+A galaxies are associated with known extended X-ray sources in the Boötes field (Kenter et al. 2005). Eight (33%) of the K+A galaxies have one or more X-ray photons within $2''$ of the optical position, including five (17%) K+A galaxies with two or more X-ray photons. For comparison, 995 of the 6592 (15%) AGES galaxies have one or more X-ray photons within $2''$ of the optical position, with 316 (5%) having two or more X-ray photons. K+A galaxies are thus more likely to harbor X-ray sources than the overall galaxy population.

We determined fraction of K+A galaxies with spurious X-ray counterparts by searching for X-ray photons within $2''$ of positions offset by $10''$ from the K+A galaxies. Approximately 8% of the offset positions had spurious X-ray counterparts (usually single photon detections) and we thus conclude that $\simeq 2$ of the 24 K+A galaxies also have spurious X-ray counterparts. We note that the

only X-ray source that does not lie in the AGN portion of the BPT diagram defined with the Kauffmann et al. (2003) criterion (see Figure 7) is a one photon source, and is thus likely to be spurious. This is also the only X-ray source that does not show evidence for an ongoing galaxy merger in the optical imaging.

To determine the nature of the X-ray sources, we estimated their X-ray fluxes and luminosities (or 2σ upper limits). To constrain the photon index, we determined the hardness ratio,

$$H.R. = (H - S)/(H + S), \quad (3)$$

where S and H are the photon counts in the 0.5-2.0 keV and 2.0-7.0 keV bands respectively. Using the 19 photons from the 8 K+A galaxies, we measure a hardness ratio of -0.2 ± 0.5 , corresponding to a photon index of $\Gamma = 1.0 \pm 1.0$. We used PIMMS version 3.9 (Mukai 1993) to determine the conversion from (*Chandra* Cycle 4) photon counts to unabsorbed X-ray flux, using a source photon index of $\Gamma = 1.0$ and a Galactic foreground HI column density of $1.75 \times 10^{20} \text{ cm}^{-2}$ (Stark et al. 1992). X-ray luminosities were determined using

$$L_X = 4\pi d_L^2 f_X (1+z)^{\Gamma-2}, \quad (4)$$

where d_L is the luminosity distance and f_X is the X-ray flux. Although our estimate of the photon index is highly uncertain, this has a modest impact on our luminosities as we are studying low redshift objects and our photon shot noise is large. The X-ray luminosities of our sources are plotted in Figure 8 and listed in Table 1.

We find that the X-ray luminosities of K+A galaxies are, on average, higher than those of other galaxies. The mean X-ray luminosity of K+A galaxies (determined using galaxies with and without XBoötes detections) is $1.5 \times 10^{41} \text{ erg s}^{-1}$ while the mean X-ray luminosity of other $I < 20$ AGES galaxies is $7 \times 10^{40} \text{ erg s}^{-1}$. (We caution that individual galaxies can have luminosities far higher and lower than these mean values.) The mean X-ray luminosity of K+A galaxies brighter than $M_R = -22$ is $4 \times 10^{41} \text{ erg s}^{-1}$, while other AGES galaxies with comparable absolute magnitudes have a mean X-ray luminosity of $1.9 \times 10^{41} \text{ erg s}^{-1}$. This is broadly consistent with the recent stacking analysis of Georgakakis et al. (2008), who find that the mean X-ray luminosity of $z \sim 0.8$ post-starbursts is $\sim 3 \times 10^{41} \text{ erg s}^{-1}$.

Many of the K+A galaxies with X-ray counterparts are almost certainly hosting AGNs. Several K+A galaxies have X-ray luminosities of $10^{42} \text{ erg s}^{-1}$, which is a factor of ~ 4 higher than local ultraluminous infrared galaxies that are predominantly powered by ongoing star formation (Ptak et al. 2003). Most of the K+A galaxies with X-ray counterparts would also be classified as AGNs using the BPT diagram and the empirical criterion of Kauffmann et al. (2003). As noted in §2, additional K+A galaxies hosting powerful AGNs are missing from our sample, due to our $H\alpha$ selection criterion (e.g., IRAS 14344+3451).

The X-ray luminosities of K+A galaxies are correlated with their optical luminosities. Five of the eight K+A galaxies brighter than $M_R = -22$ have counterparts in the *Chandra* imaging, with three having X-ray luminosities on the order of $10^{42} \text{ erg s}^{-1}$. K+A galaxies that are fainter than $M_R = -22$ have X-ray luminosities between $10^{40} \text{ erg s}^{-1}$ and $10^{41} \text{ erg s}^{-1}$, or have upper limits consistent with this luminosity range. The X-ray luminosities of K+A galaxies could be proportional to their optical luminosities, although steeper relationships are also consistent with our observations.

The most luminous K+A galaxies are frequently undergoing mergers and show strong evidence for hosting AGNs, including powerful X-ray emission. Many of the faintest K+A galaxies do not show evidence for ongoing mergers nor AGN activity. Perhaps AGN activity is weak or brief in the faintest K+A galaxies, so it is difficult to observe. Alternatively, we can conclude that the fraction of K+A galaxies that have hosted powerful AGNs and undergone mergers does increase with optical luminosity. If this is the case, perhaps two mechanisms are responsible for the truncation of star formation, with one being correlated with galaxy mergers and AGN activity. Yan et al. (2008) also conclude that there may be two mechanisms for producing K+A galaxies, after noting a bimodality in the distribution of K+A environ-

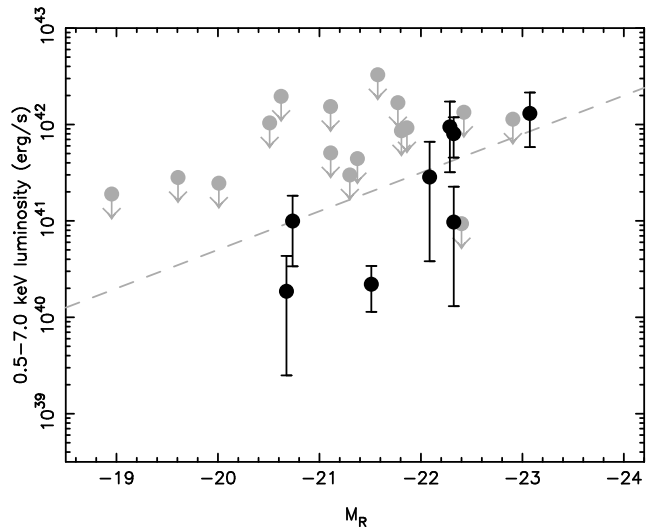


Fig. 8.— The X-ray luminosities of K+A galaxies. The *Chandra* exposure times vary by an order of magnitude, so our uncertainties and 2σ upper limits vary accordingly. As we are using a flux limited sample, there is a correlation between absolute magnitude and limiting X-ray luminosity. We expect ~ 2 spurious X-ray counterparts in the sample, and that these sources will be single photon detections. The dashed line denotes the trend expected if X-ray luminosity divided by optical luminosity is constant. Five of the eight K+A galaxies with absolute magnitudes brighter than $M_R = -22$ have X-ray counterparts, and at least three have X-ray luminosities on the order of $10^{42} \text{ erg s}^{-1}$. These powerful X-ray sources are almost certainly AGNs.

ments. Multiple mechanisms for the truncation of star formation are also found in recent semi-analytic models (e.g., Bower et al. 2006; Croton et al. 2006), with AGN feedback only playing a major role in central galaxies while other mechanisms regulate star formation in satellite and low luminosity galaxies, although how accurately these models mimic galaxy evolution remains a matter of vigorous debate.

6. SUMMARY

We have examined the AGN content of K+A galaxies, using 24 K+A galaxies selected from AGES spectroscopy of 7.9 deg² of the Boötes field. Using deep optical imaging from the NDWFS, we find that two thirds of K+A galaxies are likely ongoing mergers or are recent merger remnants. As the merger of two galaxies (initially separated by ~ 30 kpc) can take as long as a billion years, it is plausible that the mechanism that truncates star formation is triggered by galaxy mergers or that we are observing the aftermath of merger triggered bursts of star formation.

Between $z = 1$ and $z = 0$ the stellar mass contained within the red galaxy population doubles, due to the transfer of stellar mass from the blue star forming galaxy population to the red passive galaxy population. As the star formation rates of galaxies decline and they move towards the red galaxy population, their rest-frame optical colors will fall between the red and blue populations. While the optical colors of K+A galaxies fall between the red and blue populations, they represent just 1% of the $z \sim 0.2$ galaxies with these optical colors. We thus conclude that, compared to most galaxies moving from the blue population to the red population, the truncation of star formation in K+A galaxies may be unusually abrupt.

We find that K+A galaxies frequently host AGNs. Half of the K+A galaxies in our sample have emission-line ratios comparable to those of Seyferts and LINERs, while a quarter have counterparts in the *Chandra* XBoötes survey. While not direct evidence for AGN feedback, it is consistent with AGN feedback being responsible for the truncation or regulation of star formation in some galaxies.

The fraction of K+A galaxies that show clear evidence of hosting an AGN increases with optical luminosity. While most K+A galaxies have optical emission-line ratios consistent with AGNs, the faintest K+A galaxies have emission-line ratios consistent with those produced by a stellar population. A third of $M_R < -22$ K+A galaxies have X-ray counterparts with luminosities of $\sim 10^{42}$ erg s⁻¹, while it is rare for optically faint K+A galaxies to have X-ray counterparts. It is possible that the faintest K+A galaxies host short lived or very faint AGNs, which are not detected by XBoötes and are swamped by starlight and nebular emission in optical spectra. Alternatively, we speculate that two mechanisms may be responsible for truncating star formation in K+A galaxies, with AGNs truncating star formation in the most luminous galaxies while another mechanism

truncates star formation in lower luminosity galaxies.

We thank our colleagues on the AGES, NDWFS, and XBoötes teams. This paper would not have been possible without the efforts of the *Chandra*, KPNO, and MMT support staff. David Palamara's involvement in this paper began during his studies for Monash University's PHS3360 unit, which was coordinated by John Cashion. Late in the development of this work, Richard Cool was supported by NASA through Hubble Fellowship grant HST-HF-01217.01, awarded by the Space Telescope Science Institute, which is operated by the Association of Universities for Research in Astronomy, for NASA, under the contract NAS 5-26555. John Moustakas received support from NASA grant 06-GALEX06-0030 and Spitzer grant G05-AR-50443 during the development of this paper. Spectroscopic observations reported here were obtained at the MMT Observatory, a joint facility of the Smithsonian Institution and the University of Arizona. This work made use of optical images provided by the NOAO Deep Wide-Field Survey (Jannuzi & Dey 1999), which is supported by the National Optical Astronomy Observatory (NOAO). NOAO is operated by AURA, Inc., under a cooperative agreement with the National Science Foundation.

REFERENCES

- Baldwin, J. A., Phillips, M. M., & Terlevich, R. 1981, *PASP*, 93, 5
- Balogh, M. L., & Morris, S. L. 2000, *MNRAS*, 318, 703
- Barger, A. J., Cowie, L. L., Mushotzky, R. F., & Richards, E. A. 2001, *AJ*, 121, 662
- Bell, E. F., Wolf, C., Meisenheimer, K., Rix, H.-W., Borch, A., Dye, S., Kleinheinrich, M., Wisotzki, L., et al. 2004, *ApJ*, 608, 752
- Boroson, T. A., & Oke, J. B. 1984, *ApJ*, 281, 535
- Bower, R. G., Benson, A. J., Malbon, R., Helly, J. C., Frenk, C. S., Baugh, C. M., Cole, S., & Lacey, C. G. 2006, *MNRAS*, 370, 645
- Boylan-Kolchin, M., Ma, C.-P., & Quataert, E. 2008, *MNRAS*, 383, 93
- Brand, K., Brown, M. J. I., Dey, A., Jannuzi, B. T., Kochanek, C. S., Kenter, A. T., Fabricant, D., Fazio, G. G., et al. 2006, *ApJ*, 641, 140
- Brotherton, M., Diamond-Stanic, A., vanden Berk, D., Burton, R., & Croom, S. 2004, in *Astronomical Society of the Pacific Conference Series*, Vol. 311, AGN Physics with the Sloan Digital Sky Survey, ed. G. T. Richards & P. B. Hall, 285–+
- Brotherton, M. S., van Breugel, W., Stanford, S. A., Smith, R. J., Boyle, B. J., Miller, L., Shanks, T., Croom, S. M., et al. 1999, *ApJ*, 520, L87
- Brown, M. J. I., Dey, A., Jannuzi, B. T., Brand, K., Benson, A. J., Brodwin, M., Croton, D. J., & Eisenhardt, P. R. 2007, *ApJ*, 654, 858

- Brown, M. J. I., Zheng, Z., White, M., Dey, A., Jannuzi, B. T., Benson, A. J., Brand, K., Brodwin, M., et al. 2008, *ApJ*, 682, 937
- Bruzual, G., & Charlot, S. 2003, *MNRAS*, 344, 1000
- Coleman, G. D., Wu, C.-C., & Weedman, D. W. 1980, *ApJS*, 43, 393
- Couch, W. J., & Sharples, R. M. 1987, *MNRAS*, 229, 423
- Croton, D. J., Springel, V., White, S. D. M., De Lucia, G., Frenk, C. S., Gao, L., Jenkins, A., Kauffmann, G., et al. 2006, *MNRAS*, 365, 11
- Dekel, A., & Birnboim, Y. 2006, *MNRAS*, 368, 2
- Dressler, A., & Gunn, J. E. 1983, *ApJ*, 270, 7
- Efstathiou, G. 2000, *MNRAS*, 317, 697
- Faber, S. M., Willmer, C. N. A., Wolf, C., Koo, D. C., Weiner, B. J., Newman, J. A., Im, M., Coil, A. L., et al. 2007, *ApJ*, 665, 265
- Fabian, A. C., Sanders, J. S., Allen, S. W., Crawford, C. S., Iwasawa, K., Johnstone, R. M., Schmidt, R. W., & Taylor, G. B. 2003a, *MNRAS*, 344, L43
- Fabian, A. C., Sanders, J. S., Crawford, C. S., Conselice, C. J., Gallagher, J. S., & Wyse, R. F. G. 2003b, *MNRAS*, 344, L48
- Fabricant, D. G., Hertz, E. N., Szentgyorgyi, A. H., Fata, R. G., Roll, J. B., & Zajac, J. M. 1998, in *Proc. SPIE Vol. 3355*, p. 285-296, *Optical Astronomical Instrumentation*, Sandro D'Odorico; Ed., 285-296
- Franx, M. 1993, *ApJ*, 407, L5
- Fukugita, M., Nakamura, O., Turner, E. L., Helmboldt, J., & Nichol, R. C. 2004, *ApJ*, 601, L127
- Gallagher, S. C., Brandt, W. N., Chartas, G., Garmire, G. P., & Sambruna, R. M. 2002, *ApJ*, 569, 655
- Georgakakis, A., Nandra, K., Yan, R., Willner, S. P., Lotz, J. M., Pierce, C. M., Cooper, M. C., Laird, E. S., et al. 2008, *MNRAS*, 385, 2049
- Heckman, T. M. 1980, *A&A*, 87, 152
- Helmboldt, J. F., Walterbos, R. A. M., & Goto, T. 2008, *MNRAS*, 387, 1537
- Hogg, D. W., Masjedi, M., Berlind, A. A., Blanton, M. R., Quintero, A. D., & Brinkmann, J. 2006, *ApJ*, 650, 763
- Hopkins, P. F., Hernquist, L., Cox, T. J., Di Matteo, T., Robertson, B., & Springel, V. 2006a, *ApJS*, 163, 1
- Hopkins, P. F., Hernquist, L., Cox, T. J., Robertson, B., & Springel, V. 2006b, *ApJS*, 163, 50
- Jannuzi, B. T., & Dey, A. 1999, in *ASP Conf. Ser. 191: Photometric Redshifts and the Detection of High Redshift Galaxies*, ed. R. Weymann, L. Storrie-Lombardi, M. Sawicki, & R. Brunner, 111
- Kauffmann, G., Heckman, T. M., Tremonti, C., Brinchmann, J., Charlot, S., White, S. D. M., Ridgway, S. E., Brinkmann, J., et al. 2003, *MNRAS*, 346, 1055
- Kenter, A., Murray, S. S., Forman, W. R., Jones, C., Green, P., Kochanek, C. S., Vikhlinin, A., Fabricant, D., et al. 2005, *ApJS*, 161, 9
- Kewley, L. J., Dopita, M. A., Sutherland, R. S., Heisler, C. A., & Trevena, J. 2001, *ApJ*, 556, 121
- Kurucz, R. L. 1992, in *IAU Symposium, Vol. 149, The Stellar Populations of Galaxies*, ed. B. Barbuy & A. Renzini, 225-+
- Larson, R. B., Tinsley, B. M., & Caldwell, C. N. 1980, *ApJ*, 237, 692
- Liu, C. T., & Kennicutt, Jr., R. C. 1995, *ApJ*, 450, 547
- Moustakas, J., & Kennicutt, Jr., R. C. 2006, *ApJS*, 164, 81
- Mukai, K. 1993, *Legacy*, vol. 3, p.21-31, 3, 21
- Murray, S. S., Kenter, A., Forman, W. R., Jones, C., Green, P. J., Kochanek, C. S., Vikhlinin, A., Fabricant, D., et al. 2005, *ApJS*, 161, 1
- Murray, S. S., & XBootes Team. 2006, in *Bulletin of the American Astronomical Society, Vol. 38, Bulletin of the American Astronomical Society*, 1170-+
- Nolan, L. A., Dunlop, J. S., Kukula, M. J., Hughes, D. H., Boroson, T., & Jimenez, R. 2001, *MNRAS*, 323, 308
- Ptak, A., Heckman, T., Levenson, N. A., Weaver, K., & Strickland, D. 2003, *ApJ*, 592, 782
- Quintero, A. D., Hogg, D. W., Blanton, M. R., Schlegel, D. J., Eisenstein, D. J., Gunn, J. E., Brinkmann, J., Fukugita, M., et al. 2004, *ApJ*, 602, 190
- Roll, J. B., Fabricant, D. G., & McLeod, B. A. 1998, in *Proc. SPIE Vol. 3355*, p. 324-332, *Optical Astronomical Instrumentation*, Sandro D'Odorico; Ed., 324-332
- Silk, J., & Rees, M. J. 1998, *A&A*, 331, L1
- Spergel, D. N., Bean, R., Doré, O., Nolta, M. R., Bennett, C. L., Dunkley, J., Hinshaw, G., Jarosik, N., et al. 2007, *ApJS*, 170, 377
- Stark, A. A., Gammie, C. F., Wilson, R. W., Bally, J., Linke, R. A., Heiles, C., & Hurwitz, M. 1992, *ApJS*, 79, 77
- Taylor, J. E., & Babul, A. 2001, *ApJ*, 559, 716
- Tran, K.-V. H., Franx, M., Illingworth, G. D., van Dokkum, P., Kelson, D. D., & Magee, D. 2004, *ApJ*, 609, 683
- Tremonti, C. A., Moustakas, J., & Diamond-Stanic, A. M. 2007, *ApJ*, 663, L77
- Wang, J. X., Malhotra, S., Rhoads, J. E., Brown, M. J. I., Dey, A., Heckman, T. M., Jannuzi, B. T., Norman, C. A., et al. 2004, *AJ*, 127, 213
- Wild, V., Walcher, C. J., Johansson, P. H., Tresse, L., Charlot, S., Pollo, A., Le Fèvre, O., & de Ravel, L. 2009, *MNRAS*, 395, 144
- Worthey, G., & Ottaviani, D. L. 1997, *ApJS*, 111, 377
- Wyithe, J. S. B., & Loeb, A. 2003, *ApJ*, 595, 614

- Yan, R., Newman, J. A., Faber, S. M., Coil, A. L., Cooper, M. C., Davis, M., Weiner, B. J., Gerke, B. F., et al. 2008, ArXiv e-prints, 805
- Yan, R., Newman, J. A., Faber, S. M., Konidaris, N., Koo, D., & Davis, M. 2006, ApJ, 648, 281
- Yang, Y., Tremonti, C. A., Zabludoff, A. I., & Zaritsky, D. 2006, ApJ, 646, L33
- Yang, Y., Zabludoff, A. I., Zaritsky, D., & Mihos, J. C. 2008, ApJ, 688, 945
- York, D. G., Adelman, J., Anderson, J. E., Anderson, S. F., Annis, J., Bahcall, N. A., Bakken, J. A., Barkhouser, R., et al. 2000, AJ, 120, 1579
- Zabludoff, A. I., Zaritsky, D., Lin, H., Tucker, D., Hashimoto, Y., Shectman, S. A., Oemler, A., & Kirshner, R. P. 1996, ApJ, 466, 104
- Zaritsky, D., Zabludoff, A. I., & Willick, J. A. 1995, AJ, 110, 1602

TABLE 1
BOÖTES K+A GALAXY SAMPLE, ORDERED BY ABSOLUTE MAGNITUDE.

J2000 Coordinates	Redshift	I	M_R	Companion (< 30 kpc)	Tidal Tail	BPT ^b Class	X-ray Photons	X-ray Exp. (sec.)	L_X (erg s^{-1})
14:26:37.266 +34:46:25.63	0.1314	19.45	-18.95	N	N	SF	0	8943	$< 1.9 \times 10^{41}$
14:26:18.398 +35:02:48.55	0.1567	19.31	-19.61	Y	N	SF	0	8658	$< 2.8 \times 10^{41}$
14:30:14.018 +33:51:38.84	0.1817	19.01 ^a	-20.01	Y	N	SF	0	13481	$< 2.5 \times 10^{41}$
14:35:51.378 +33:33:53.72	0.2037	18.93	-20.51	N	N	?	0	4055	$< 1.0 \times 10^{42}$
14:38:11.278 +34:07:47.69	0.2641	19.52	-20.62	N	N	?	0	3694	$< 2.0 \times 10^{42}$
14:33:29.167 +33:28:21.37	0.1725	18.36	-20.68	N	N	SF	1	42306	$(1.9 \pm 2.5) \times 10^{40}$
14:29:47.738 +34:16:18.81	0.1220	17.41	-20.74	N	Y	SF/AGN	2	7722	$(1.0 \pm 0.7) \times 10^{41}$
14:38:19.445 +35:36:01.98	0.2483	18.88	-21.11	N	Y	SF/AGN	0	4141	$< 1.5 \times 10^{42}$
14:30:55.228 +33:26:01.11	0.2017	18.35	-21.11	N	Y	?	0	8126	$< 5.1 \times 10^{41}$
14:31:01.102 +34:08:44.34	0.2307	18.47	-21.30	N	N	SF	0	18232	$< 3.0 \times 10^{41}$
14:25:52.846 +32:55:56.05	0.2139	18.20	-21.37	N	N	?	0	10536	$< 4.4 \times 10^{41}$
14:25:48.378 +35:40:55.65	0.1840	17.66	-21.51	N	Y	SF/AGN	4	163416	$(2.2 \pm 1.2) \times 10^{40}$
14:34:39.522 +34:30:21.67	0.3411	19.19	-21.57	N	N	SF/AGN	0	3773	$< 3.3 \times 10^{42}$
14:31:20.690 +35:29:26.20	0.3347	19.00	-21.77	Y	N	SF/AGN	0	7068	$< 1.7 \times 10^{42}$
14:29:59.370 +34:22:41.67	0.2655	18.41	-21.81	N	N	AGN	0	8511	$< 8.6 \times 10^{41}$
14:35:00.640 +33:29:23.18	0.2736	18.33	-21.86	Y	N	SF/AGN	0	8430	$< 9.3 \times 10^{41}$
14:25:42.236 +32:44:08.47	0.2079	17.47	-22.09	N	Y	SF/AGN	1	4078	$(2.8 \pm 3.8) \times 10^{41}$
14:34:54.275 +33:00:59.97	0.2986	18.22	-22.29	N	N	?	2	5239	$(9.5 \pm 7.5) \times 10^{41}$
14:25:39.281 +33:56:44.48	0.3085	18.20	-22.32	Y	Y	SF/AGN	5	16506	$(8.0 \pm 3.9) \times 10^{41}$
14:29:26.729 +33:48:30.14	0.2417	17.56	-22.32	Y	Y	SF/AGN	1	16328	$(9.7 \pm 8.4) \times 10^{40}$
14:31:46.450 +34:17:18.49	0.1234	15.80	-22.40	N	Y	AGN	0	15953	$< 9.4 \times 10^{40}$
14:34:31.800 +33:47:59.17	0.3318	18.31	-22.42	Y	N	SF/AGN	0	8725	$< 1.3 \times 10^{42}$
14:25:44.882 +33:34:31.20	0.3011	17.59	-22.91	Y	Y	AGN	0	8391	$< 1.1 \times 10^{42}$
14:26:21.757 +35:11:47.37	0.3461	17.85	-23.07	N	Y	AGN	3	7772	$(1.3 \pm 0.7) \times 10^{42}$

^aA nearby bright star may be biasing the photometry of this galaxy.

^bAGN denotes objects above the criterion of Kewley et al. (2001). SF/AGN denoted objects between the criteria of (Kewley et al. 2001) and (Kauffmann et al. 2003). SF denotes objects below the criterion of Kauffmann et al. (2003). “?” denotes objects without significant detections in the relevant emission-lines for the BPT diagram.